proceedings

MDPI

Proceedings

Combinatory Action of Chitosan-Based Blended Films and Loaded Cajeput Oil Against Staphylococcus Aureus and Pseudomonas Aeruginosa-Mediated Infections †

Joana C. Antunes *, Tânia D. Tavares, Natália C. Homem, Marta A. Teixeira, M. Teresa P. Amorim and Helena P. Felgueiras

Centre for Textile Science and Technology (2C2T), Department of Textile Engineering, Campus of Azurém, University of Minho, 4800-058 Guimarães, Portugal; natalia.homem@2c2t.uminho.pt (N.C.H.); martaalbertinateixeira@gmail.com (M.A.T.); mtamorim@det.uminho.pt (M.T.P.A.); helena.felgueiras@2c2t.uminho.pt (H.P.F.); taniatav@2c2t.uminho.pt (T.D.T.)

* Correspondence: joana.antunes@2c2t.uminho.pt; Tel.: +351-253-510-283; Fax: +351-253-510-293

† Presented at the First International Conference on "Green" Polymer Materials 2020, 5–25 November 2020; Available online: https://cgpm2020.sciforum.net/.

Published: 4 November 2020

Abstract: Chronic wounds (CW) have numerous entry ways for pathogen invasion and prosperity, damaging host tissue and hindering tissue remodeling. Essential oils exert quick and efficient antimicrobial (AM) action, unlikely to induce bacterial resistance. Cajeput oil (CJO) has strong AM properties, namely against *Staphylococcus aureus* and *Pseudomonas aeruginosa*. Chitosan (CS) is a natural and biodegradable cationic polysaccharide, also widely known for its AM features. CS and poly (vinyl alcohol) (PVA) films were prepared (ratio 30/70; 9%wt) by solvent casting and phase inversion method. Film's thermal stability and chemical composition data reinforce polymer blending. Films were supplemented with 1 and 10wt% of CJO in relation to total polymeric mass. Loaded films were 23 and 57% thicker, respectively, than the unloaded films. Degree of swelling and porosity also increased, particularly with 10wt% CJO. AM testing revealed that CS films alone were effective against both bacteria, eradicating all *P. aeruginosa* within the hour (*** $p < 0.001$). Still, loaded CS/PVA films showed improved AM traits, being significantly more efficient than unloaded films right after 2 h of contact. This study is a first proof of concept that CJO can be dispersed into CS/PVA films and show bactericidal effects, particularly against *P. aeruginosa*, this way opening new avenues for CW therapeutics.

Keywords: bactericidal; marine-derived polymers; natural bioactive agents; drug delivery systems; blended films

1. Introduction

Diabetes Mellitus (DM) is a disabling and incurable chronic metabolic and degenerative disorder, highly prevalent in Portugal and worldwide, severely affecting patient's quality of life and demanding high healthcare costs. 71% of all global deaths are due to noncommunicable diseases (NCD), with DM having a substantial contribution to that number [1]. Non-healing diabetic foot ulcers (DFUs) are a common and costly complication of DM, leading to high limb amputation prevalence worldwide. More than half of those ulcers become infected. Recurrence is frequent, with pathogen clearance and degenerated tissue recovery being increasingly more difficult each time [2].

Current therapeutics are ineffective in breaking this detrimental chain, therefore effective solutions are needed.

Chitin is the second most abundant natural polymer in the world. It is the primary structural component of the exoskeleton of shrimps, crabs, lobster and squid pens, and present in lesser amounts in cell walls of some fungi and yeast and in plants [3]. When the degree of acetylation (DA, molar fraction of N-acetylated units) is lower than about 50%, the polymer is termed CS, carrying glucosamine and N-acetylglucosamine units connected through a β-1,4-glycosidic bond through acetal functions [4,5]. CS is a nontoxic and a biologically compatible polymer, fit for multiple biomedical applications such as wound dressing. CS's molecular weight (M_w) and the degree of acetylation (DA) are its main structural parameters influencing the overall behavior of the polymer as a biomaterial, which include mucoadhesive, chemoattractive, analgesic, hemostatic, antibacterial and antifungal action (among others) [3]. It is typically combined with other compounds for improved mechanical strength and increased applicability [3,5]. In parallel, renewable plant-derived products with antimicrobial properties are increasingly considered as an alternative to antibiotics [6]. Essential oils (EOs), in particular, are aromatic, volatile, lipophilic biomolecules, extracted from regions of plants (e.g., flowers, leaves, twigs, bark, wood, fruits, etc.), in which they work as secondary metabolites, defending the host from microbial invasion [6,7]. EO's composition-including the hydrophobic thymol, carvacrol and eugenol (among others)-exhibit a broad spectrum of antimicrobial activity against bacteria, fungi, and viruses [8]. Still, their cytotoxicity at increased concentrations, their low resistance to degradation by external factors (e.g., temperature, light, moisture), and their volatility in their free, liquid form hinder their expanded use.

Bioactive dressings for DFU treatment that incorporate natural AM agents in their formulation have been suggested as an alternative to the set of clinically-approved conventional approaches [7]. In the present work, we propose to engineer a 3D film via solvent casting and phase-inversion from CS and poly(vinyl alcohol) (PVA) blends, polymers widely combined as templates for AM action [9–11], and loaded with the antibacterial cajeput (CJO) EO while aiming at an improved control of infections governed by *Staphylococcus aureus* and *Pseudomonas aeruginosa* (the most prevalent bacteria within infected DFUs [12]). The main goal is to explore the potential of CS and CJO synergistic effect over microbial growth inhibition, within a matrix with the flexible and hydrophilic PVA, for prospective CW treatments.

2. Experiments

2.1. Materials

Chitosan (CS, Mw = 100–300 kDa; Acros Organics, Fair Lawn, NJ, USA) and polyvinyl alcohol (PVA, Mw = 72 kDa, 88% hydrolysed; Polysciences, Inc., Warrington, PA, USA) were used to produce the blended films. A DA of 9.6 ± 1.4% was determined for CS by Fourier transform infrared spectroscopy (FTIR) spectrum with KBr pellets, through the method proposed by Brugnerotto et al. [13]. Aqueous solutions of glacial acetic acid (AA, Fisher Scientific, Waltham, MA, USA) and distilled water (dH_2O) were used as solvents for CS and PVA, respectively. Sodium hydroxide (NaOH) and sodium sulfate (Na_2SO_4) were both acquired from Merck and included in the coagulation bath of the blends.

Cajeput EO (CJO), an EO from *Melaleuca leucadendron*, was purchased from Folha d'Água Company (Portugal), having a density of 0.911 g/cm^3. Trypticase soy broth (TSB), trypticase soy agar (TSA), nutrient broth (NB) and nutrient agar (NA) were acquired from VWR, while Mueller Hinton broth (MHB) was obtained from CondaLab. Bacteria were supplied from American Type Culture Collection (ATCC), encompassing Gram-positive bacteria, *S. aureus* (ATCC 6538) and Gram-negative bacteria, *P. aeruginosa* (ATCC 25853). The EO was selected based on results obtained elsewhere by the team [14,15]. The MIC value for each CJO/bacteria combination was established as the concentration at which bacteria did not show any growth, determined visually, and confirmed by the differences in absorbance readings. Existence of viable cells at MIC and at concentrations in its vicinity (concentration higher and lower than MIC value) was determined by measuring the number of

CFUs/mL. MICs of 45.6 mg/mL were obtained by the team, for both *S. aureus* and *P. aeruginosa* reference strains.

2.2. CS/CJO/PVA Film Production

CS and PVA films were prepared by solvent casting and phase inversion method [3]. 4% CS solution in 1% acetic acid were added to 19% PVA solution (in distilled water, dH_2O, at 80 °C), stirred and casted in glass Petri dishes (d = 14 cm). After drying at 40 °C (24–72 h) to remove excess of solvent, a coagulation bath with 8% NaOH and 2% Na_2SO_4 neutralized and detached built films in 24 h. Films were kept in the later bath at 4 °C, being washed 3 times with dH_2O (with orbital shaking at 50 rpm for 5 min each time) right before each characterization method. CJO-loaded films were obtained following CJO incorporation within the CS solution 5 min before blending. EO was added at the necessary volume to give rise to a concentration of 1 or 10% (w/w) CJO in regard to the total polymeric mass (specifically 35.1 or 351 mg within 3.51 g of CS and/or PVA). Figure 1 illustrates the main steps taken to produce the films, while Table 1 highlights each of the built film processing conditions, along with CS/PVA mass ratios.

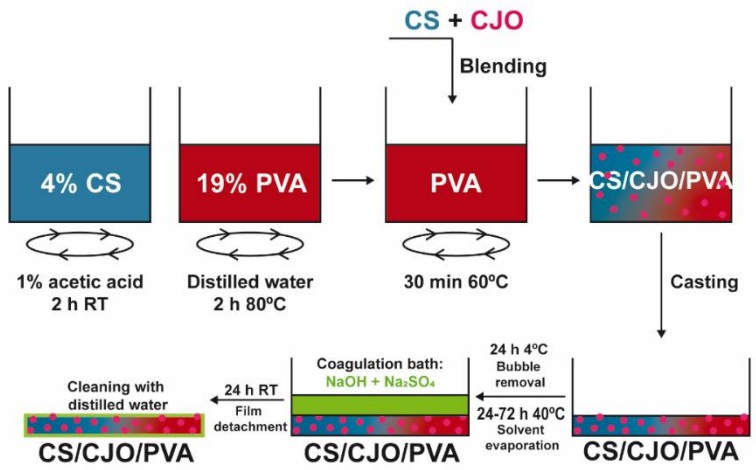

Figure 1. Preparation of CJO-loaded CS/PVA blended films. Films were prepared through solvent casting followed by phase inversion method. After separate polymer dissolution in an adequate solvent, CJO was added at 1/10%wt in relation total polymeric mass to CS solution, stirred for 10 min, and blended with PVA. Casted mix was refrigerated for bubble removal, heated for solvent evaporation, and neutralized with salt ions in a suitable amount to induce film detachment from the glass. After cleaning in dH_2O, the loaded CS/CJO/PVA films were obtained.

Table 1. Practical numbers required to build tested CS/CJO/PVA blended films, specifically CJO loading amount (in μL), mass (g) and volume (mL) of polymer solutions for each case, total mass percent (%m/V), total volume (mL) and selected CS/PVA mass ratios.

	EO		**CS Solution**		**PVA Solution**		**Total %w/V**	**V_{Total} (mL)**	**CS/PVA Mass Ratios**
	m (mg)	**V (μL)**	**m_{CS} (g)**	**V (mL)**	**m_{PVA} (g)**	**V (mL)**			
CS	-	-	3.51	39	-	-			100/0
PVA	-	-	-	-	3.51	39			0/100
CS/PVA	-	-							
CS/PVA/CJO 1%	35.1	39.2	1.053	26	2.457	13	9%	39	30/70
CS/PVA/CJO 10%	351	392							

2.3. Physical and Chemical Characterization

2.3.1. Macroscopic Assessment

A representative photo of the macroscopic view of the created films is displayed in Figure 2a. Then, Figure 2b depicts punches of 11 mm in diameter of each film type that enabled thickness measurements, using a Mitotoyo 2046E-10 dial indicator, with resolution of 0.01 mm and 10 mm pressing area. Film's wet weight (in mg) was registered, with excess of dH_2O on the surface of the films eliminated using kimwipes (Kimtech) prior to weighting, and dried for 7 days at 37 °C, moment at which films' mass reached a constant value. The films' degree of swelling (DS, in %) was determined by measuring the weight of the samples before and after drying, similarly as previously performed by Felgueiras et al. [7]. It was calculated using the following Equation (1):

$$\mathrm{DS}(\%) = \frac{\mathrm{m_w} - \mathrm{m_d}}{\mathrm{m_w}} \times 100, \quad (1)$$

where m_w (mg) is the weight of the wet film, m_d (mg) is the weight of the dry film

The films porosity (ϵ) was also determined by measuring the mass loss after drying, through the Equation (2):

$$\varepsilon = \frac{m_w - m_d}{AL\rho}, \quad (2)$$

where and A, L, and ϱ are the wet film effective area (cm^2), the wet film thickness (cm), and the dH_2O density (g/cm^3), respectively.

2.3.2. Thermal Properties

Thermal gravimetric analysis (TGA) measurements were conducted on a STA 449 F3 from NETZSCH Q500 using a platinum pan. The TGA trace was obtained in the range of 25–700 °C under nitrogen atmosphere, flow rate of 200 mL/min, and temperature rise of 10 °C/min. Results were plotted as percentage of weight loss/derivative of glass transition temperature (DTG) vs. temperature.

2.3.3. Chemical Composition

Films chemical composition (FTIR with attenuated total reflection—FTIR-ATR) on dried films (7 d at 37 °C) was evaluated using an IRAffinity-1S, SHIMADZU spectrophotometer (Kyoto, Japan), with an ATR accessory (diamond crystal). For each sample, a total of 200 scans were performed at a spectral resolution of 2 cm^{-1}, over the wavenumber range of 400–4000 cm^{-1}.

2.4. Antimicrobial Action

2.4.1. Time Kill Kinetics

Bacteria suspensions were prepared at 1×10^5 CFUs/mL in TSB (*S. aureus*) and NB (*P. aeruginosa*) and combined with the all prepared films. Control groups were prepared without film addition. Bacteria-containing solutions were incubated at 37 °C and 120 rpm. After 0 (before action), 1, 2, 6 and 24 h of incubation, bacteria were serially diluted (10^1 to 10^5 in PBS), cultured on TSA/NA plates and further incubated for another 24 h at 37 °C. Colonies of surviving bacteria were counted and reported as mean ± standard deviation (S.D.). Log reduction determinations were also conducted between bacteria solutions with and without antimicrobial agents and fibers unloaded and loaded.

2.4.2. Statistical Analysis

Statistical analysis was performed using GraphPad Prism (version: 7.04). The parametric distribution of the data was first evaluated by the D'Agostino-Pearson omnibus normality test. Because the data followed a non-parametric distribution, statistical analysis was performed with the Kruskal-Wallis test, followed by the Dunn's multiple comparisons test, to compare each unpaired

group. A confidence interval of at least 95% was chosen to define statistical significance (* $p < 0.05$, ** $p < 0.005$, *** $p < 0.001$ and **** $p < 0.0001$).

3. Results and Discussion

3.1. Macroscopic Assessment

CS/PVA blended films were produced via solvent casting-phase inversion method, following adaptation to what had been previously optimized by the team [7]. Macroscopically homogeneous films with 0.72 ± 0.02 mm of thickness, 85.22 ± 2.93% of DS and 89.52 ± 4.62 of porosity were obtained, apart from occasional defects related to retained air bubbles. CJO loading tended to increase film thickness up to 124 or 158%, respectively, for films loaded with 1 or 10% CJO in relation to total polymeric mass of CS and PVA. The occurrence of less compact films suggests an alteration of the polymeric chain distribution and bonding opportunities [7]. Indeed, a slight increment of overall water retention capacity, and porosity, has been observed, following the hydrophobic CJO entrapment within the blended matrix.

(a)

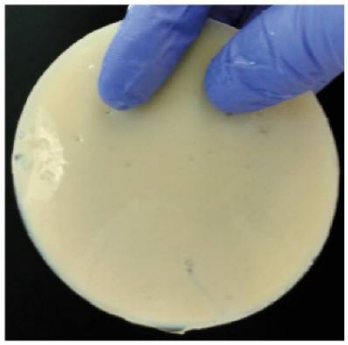

(b)

	Thickness (mm)	Degree of Swelling (%)	Porosity
CS	1.73 ± 0.11**	87.45 ± 6.04	87.44 ± 3.68
PVA	0.47 ± 0.06	72.01 ± 6.68	76.42 ± 8.91
CS/PVA	0.72 ± 0.02	85.22 ± 2.93	89.52 ± 4.62
CS/PVA/CJO 1%	0.89 ± 0.05	85.87 ± 1.18	90.15 ± 4.34
CS/PVA/CJO 10%	1.14 ± 0.10	88.50 ± 1.74	91.83 ± 5.25

Figure 2. Macroscopic assessment of CS/PVA-based blended films. (**a**) Output created through the adapted solvent casting-phase inversion method, with overview hereby represented by the CS film; and (**b**) direct measure of the films' thickness (mm) with a dial indicator (resolution of 0.01 mm and 10 mm pressing area), and indirect quantification of degree of swelling (%) and porosity through gravimetry. Results are shown as mean ± SD (n = 4 punched films with 11 mm of diameter each, cut from each film's periphery to its centre). ** $p < 0.005$ in comparison to the CS/PVA film, using the Kruskal-Wallis test, followed by the Dunn's multiple comparisons test.

3.2. Thermal Properties

Degradation steps resulting from temperature rising were evaluated via TGA and DTG (Figure 3). CS has a main degradation peak at 281 °C, showing a high residual weight (34.07%) after all the heating steps. PVA films, on the other hand, exhibit three main degradation steps: the second degradation step detected at 269 °C was attributed to the cleavage of the PVA polymeric backbone, which initiates with the degradation of the side chains and progresses to the main chain scission (368 °C) until only carbon char remains (3.20% of residual mass at 700 °C). CS/PVA-related curves display contribution of both CS and PVA's thermal features, corroborating the achievement of CS/PVA blended films, carrying lower thermal resistance than PVA films alone. A prominent degradation peak could be clearly perceived at 279 °C with 18.48% of sample remaining after heating up to the 700 °C. Films enriched with CJO present a thermal-induced behavior remarkably similar to the one observed in the unloaded films. The antimicrobial agents influence appears to be neglectable.

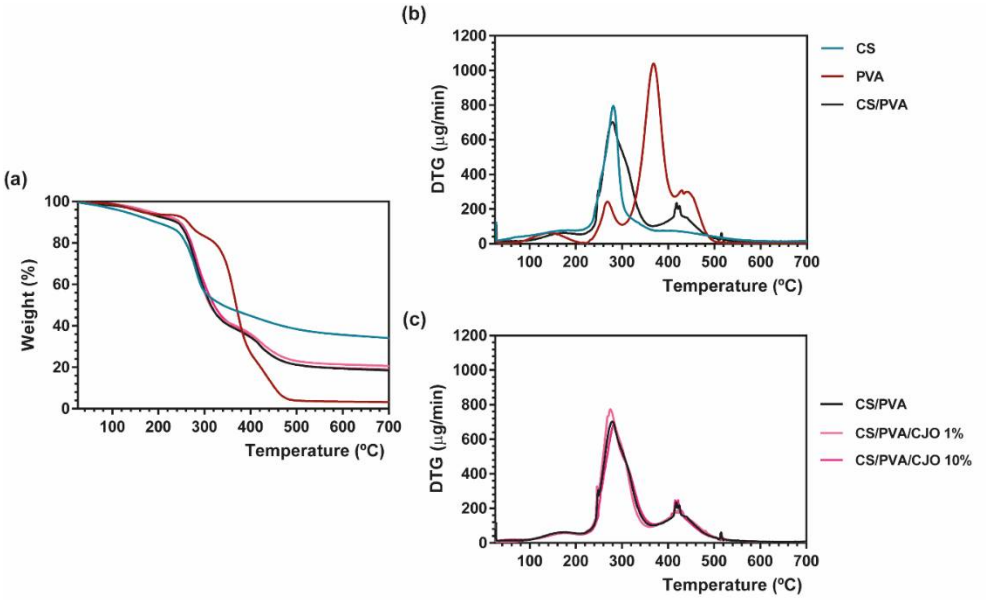

Figure 3. Representative TGA (**a**) and DTG (**b**,**c**) curves of CJO-unloaded and loaded CS/PVA-based blended films from 25 to 700 °C, performed at a heating rate of 10 °C/min in a nitrogen atmosphere.

3.3. Chemical Composition

The characteristic saccharide peaks of CS in the 945−1190 cm^{-1} region can be observed, namely the C−O stretching absorption band at 1063 and 1027 cm^{-1} and the C−O−C asymmetric stretching vibrations at ~1151 cm^{-1}. The N−H scissoring deformation peak at 1594 cm^{-1}, indicative of the presence of saturated primary amine groups, is also evident in the spectrum curves. Also within the highlighted region, PVA absorbs distinctively at 1088 cm^{-1} (C=O stretching vibrations), additionally displaying CH_2 bending vibrations at around 850 cm^{-1}. CS/PVA's chemical fingerprint shows peaks from both CS and PVA, and new peaks are absent, thereby suggesting the occurrence of polymers blend. However, in line with TGA and DTG linings, FTIR spectra did not suffer substantial changes on account of CJO incorporation. Strong interactions due to hydrogen bond formation between amino and hydroxyl groups of CS and PVA lead to partial miscibility of PVA and CS in the blend film, with increased hydrophilicity and mechanical properties (in comparison to CS films alone) as well as improved stability of PVA in aqueous environments [9–11]. A wide adsorption peak between 3400 and 3200 cm^{-1}, observed on all films even after drying, corresponded to the stretching vibrations of intermolecular hydrogen bonds of hydroxyl groups (data not shown). CJO-characteristic peaks, expected at 1577 and 1543 cm^{-1} (assigned to the aromatic ring C=C skeleton vibration of an aromatic substance) [14] were possibly undetected in these spectra due to bands overlap.

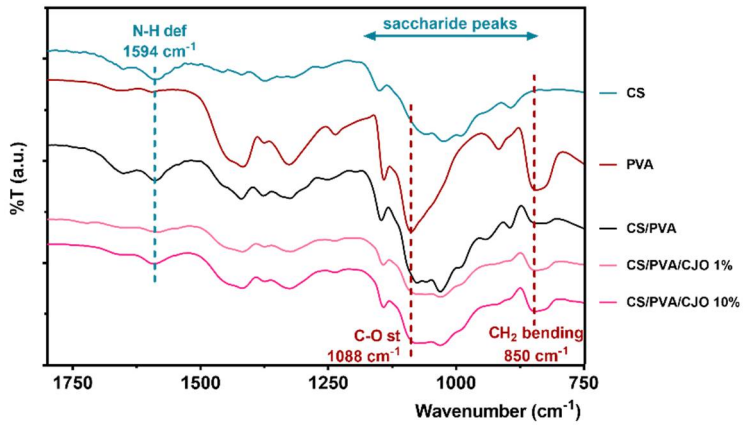

Figure 4. FTIR-ATR spectra of the CJO-unloaded and loaded CS/PVA-based blended films (4000–400 cm^{-1}). As the most significant for this study, the section between 1800–750 cm^{-1} was amplified for a clearer detection of the most relevant peaks.

3.4. Antimicrobial Action

Time Kill Kinetics

Films created with 100% CS or comprising 30% CS, 70% PVA and 1/10% CJO were capable of invoking a higher AM activity than the control without any agents, as expected. CS films, however, were the most effective from the group, exerting a quicker and stronger action against each of the bacterium, being able to completely eliminate *P. aeruginosa* during the first hour of incubation. Films impregnated with CJO at 10%wt were the most effective from the group, revealing a powerful synergistic effect of the EO and CS-based films in the battle for infection control for chronic wound care. The attractive AM activity of CS is hereby confirmed. Indeed, isolated reports are available on the use of combinations of antibiotics and CS and its derivates as antimicrobials. *P. aeruginosa*, notably, is often resistant to most antimicrobial agents. However, combinatory therapies have been proven successful to overcome the antibiotic crisis [16].

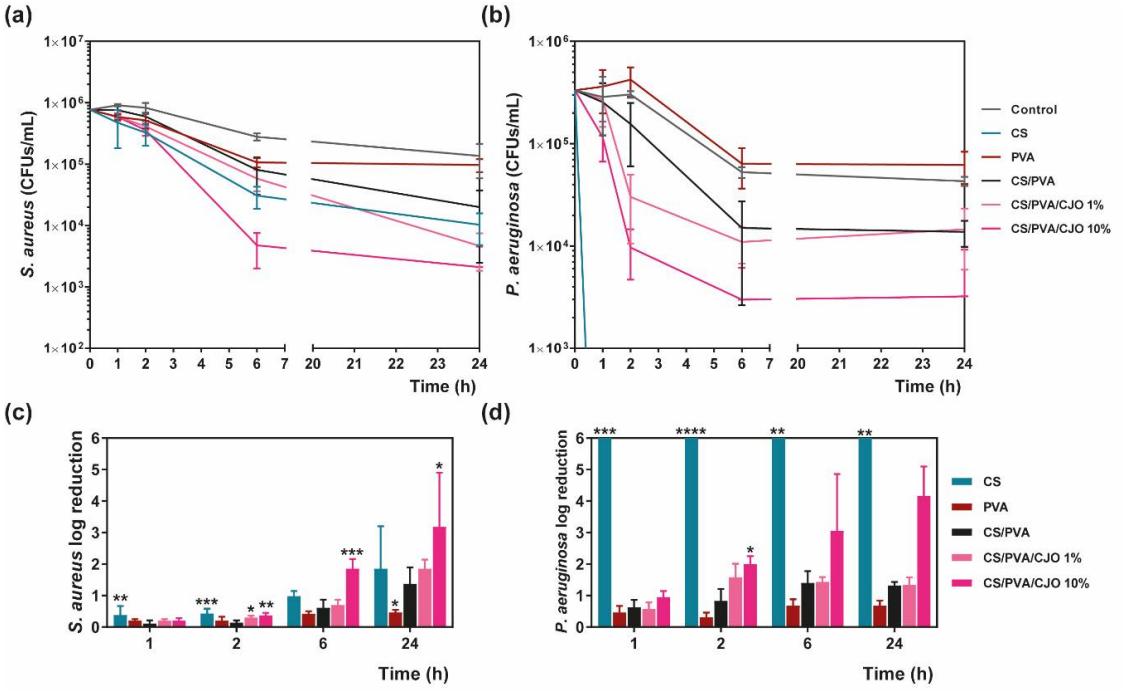

Figure 5. Killing-time curves of CS, PVA, CS/PVA and CJO-loaded CS/PVA films, against *S. aureus* (**a**) and *P. aeruginosa* (**b**) bacteria, up to 24 h of culture. Data derived from three repetitions. Positive controls for each bacterium (growth without antimicrobial agent or film) were also conducted. (**c**) *S. aureus* and (**d**) *P. aeruginosa* reduction (calculated as log reduction) in relation to control samples, namely bacterial inoculum without antimicrobial agent and unloaded films (n = 3, mean ± S.D.). The elimination of 100% of bacteria was considered as log 6. * $p < 0.05$, ** $p < 0.005$, *** $p < 0.001$ and **** $p < 0.0001$ in comparison to the CS/PVA film, using the Kruskal-Wallis test, followed by the Dunn's multiple comparisons test.

4. Conclusions

In summary, CS/PVA films supplemented with CJO showed efficient bactericidal effects following 2 h of direct contact with the infected microenvironments, being significantly more efficient than unloaded films. Films built solely of CS were even more effective than 10% CJO-loaded films in the fight against *S. aureus* and *P. aeruginosa*'s survival and prosperity. Future work will be directed towards a balance between AM action of CS and its mechanical hindrance after processing, together with the combination with CJO to an intensified antimicrobial profile against both bacteria.

Author Contributions: conceptualization, J.C.A., H.P.F.; performing experiments, J.C.A., N.C.H., T.D.T.; writing original draft, J.C.A.; revision and editing, J.C.A., N.C.H., M.A.T., H.P.F.; supervision, M.T.P.A., H.P.F.; funding acquisition, M.T.P.A., H.P.F. All authors have read and agreed to the published version of the manuscript.

Acknowledgments: Authors acknowledge the Portuguese Foundation for Science and Technology (FCT), FEDER funds by means of Portugal 2020 Competitive Factors Operational Program (POCI) and the Portuguese Government (OE) for funding the project PEPTEX with reference PTDC/CTM-TEX/28074/2017 (POCI-01-0145-FEDER-028074). Authors also acknowledge project UID/CTM/00264/2020 of Centre for Textile Science and Technology (2C2T), funded by national funds through FCT/MCTES.

Conflicts of Interest: The authors declare no conflict of interest.

References

1. Noncommunicable Diseases. Available online: http://www.who.int/mediacentre/factsheets/fs355/en/ (assessed on 19 October 2020).
2. Ramirez-Acuña, J.M.; Cardenas-Cadena, S.A.; Marquez-Salas, P.A.; Garza-Veloz, I.; Perez-Favila, A.; Cid-Baez, M.A.; Flores-Morales, V.; Martinez-Fierro, M.L. Diabetic Foot Ulcers: Current Advances in Antimicrobial Therapies and Emerging Treatments. *Antibiotics* **2019**, *8*, 193, doi:10.3390/antibiotics8040193.
3. Jc, A.; Rm, G.; Ma, B. Chitosan/Poly(γ-glutamic acid) Polyelectrolyte Complexes: From Self- Assembly to Application in Biomolecules Delivery and Regenerative Medicine. *Res. Rev. J. Mater. Sci.* **2016**, *4*, 12–36, doi:10.4172/2321-6212.1000153.
4. Kumar, M.N.R. A review of chitin and chitosan applications. *React. Funct. Polym.* **2000**, *46*, 1–27, doi:10.1016/s1381-5148(00)00038-9.
5. Rinaudo, M. Chitin and chitosan: Properties and applications. *Prog. Polym. Sci.* **2006**, *31*, 603–632, doi:10.1016/j.progpolymsci.2006.06.001.
6. Tavares, T.D.; Antunes, J.C.; Padrão, J.; Ribeiro, A.I.; Zille, A.; Amorim, M.T.P.; Ferreira, F.; Felgueiras, H.P. Activity of Specialized Biomolecules against Gram-Positive and Gram-Negative Bacteria. *Antibiotics* **2020**, *9*, 314, doi:10.3390/antibiotics9060314.
7. Felgueiras, H.P.; Teixeira, M.A.; Tavares, T.D.; Homem, N.C.; Zille, A.; Amorim, M.T.P. Antimicrobial action and clotting time of thin, hydrated poly(vinyl alcohol)/cellulose acetate films functionalized with LL37 for prospective wound-healing applications. *J. Appl. Polym. Sci.* **2019**, *137*, 48626, doi:10.1002/app.48626.
8. Omonijo, F.A.; Ni, L.; Gong, J.; Wang, Q.; Lahaye, L.; Yang, C. Essential oils as alternatives to antibiotics in swine production. *Anim. Nutr.* **2018**, *4*, 126–136, doi:10.1016/j.aninu.2017.09.001.
9. Koosha, M.; Hamedi, S. Intelligent Chitosan/PVA nanocomposite films containing black carrot anthocyanin and bentonite nanoclays with improved mechanical, thermal and antibacterial properties. *Prog. Org. Coatings* **2019**, *127*, 338–347, doi:10.1016/j.porgcoat.2018.11.028.

10. Merlusca, I.P.; Matiut, D.S.; Lisa, G.; Silion, M.; Gradinaru, L.; Oprea, S.; Popa, I.M. Preparation and characterization of chitosan–poly(vinyl alcohol)–neomycin sulfate films. *Polym. Bull.* **2017**, *75*, 3971–3986, doi:10.1007/s00289-017-2246-1.
11. Wu, Y.; Ying, Y.; Liu, Y.; Zhang, H.; Huang, J. Preparation of chitosan/poly vinyl alcohol films and their inhibition of biofilm formation against Pseudomonas aeruginosa PAO1. *Int. J. Biol. Macromol.* **2018**, *118*, 2131–2137, doi:10.1016/j.ijbiomac.2018.07.061.
12. Machado, C.; Teixeira, S.; Fonseca, L.; Abreu, M.; Carvalho, A.; Pereira, M.T.; Amaral, C.; Freitas, C.; Ferreira, L.; Neto, H.R.; et al. Evolutionary trends in bacteria isolated from moderate and severe diabetic foot infections in a Portuguese tertiary center. *Diabetes Metab. Syndr. Clin. Res. Rev.* **2020**, *14*, 205–209, doi:10.1016/j.dsx.2020.02.010.
13. Brugnerotto, J.; Lizardi, J.; Goycoolea, F.; Argüelles-Monal, W.; Desbrieres, J.; Rinaudo, M. An infrared investigation in relation with chitin and chitosan characterization. *Polymer* **2001**, *42*, 3569–3580, doi:10.1016/s0032-3861(00)00713-8.
14. Felgueiras, H.P.; Homem, N.C.; Teixeira, M.A.; Ribeiro, A.R.M.; Antunes, J.C.; Amorim, M.T.S.P. Physical, Thermal, and Antibacterial Effects of Active Essential Oils with Potential for Biomedical Applications Loaded onto Cellulose Acetate/Polycaprolactone Wet-Spun Microfibers. *Biomolecules* **2020**, *10*, 1129, doi:10.3390/biom10081129.
15. Tavares, T.D.; Antunes, J.C.; Padrão, J.; Ribeiro, A.I.; Zille, A.; Amorim, M.T.P.; Ferreira, F.; Felgueiras, H.P. Activity of Specialized Biomolecules against Gram-Positive and Gram-Negative Bacteria. *Antibiotics* **2020**, *9*, 314, doi:10.3390/antibiotics9060314.
16. Tin, S.; Sakharkar, K.R.; Lim, C.S.; Sakharkar, M.K. Activity of Chitosans in combination with antibiotics in Pseudomonas aeruginosa. *Int. J. Biol. Sci.* **2009**, *5*, 153–160, doi:10.7150/ijbs.5.153.